

PREPARATION OF NANOPARTICLES BY LASER ABLATION AT DIFFERENT WAVELENGTHS

Heba Abdulla Attia ¹

Ruqaya Mahmood Khalaf ²

M. W. Aziz ³

^{1,2,3}Department of Physics, College of Education for Women,
University of Kirkuk, Kirkuk, Iraq
hebaabdulla@uokirkuk.edu.iq
ruqayamahmood@uokirkuk.edu.iq
marwah-waleed@uokirkuk.edu.iq

Abstract:

Through laser ablation in liquid, with a Q-switch Nd:YAG laser operating at different laser energy and wavelengths, a TiO₂ NPs suspension in deionized distilled water was produced. Characterization of the materials was done using transmission electron microscopy (TEM), X-ray diffraction (XRD), and UV-visible absorption spectra obtained with a UV-visible spectrophotometer. The UV-Vis spectra, on the other hand, revealed the distinctive absorbance peak of TiO₂ NPs across bands. TiO₂NPs' estimated optical band gaps were 3.26 eV, 3.3 eV, and 3.09 eV at (250 mJ, 300 mJ) at wavelengths of 1064 nm and 532 nm, respectively. TEM pictures displayed a spherical-like form of titanium NPs with varying size distributions vary based on the different wavelengths utilized. The TiO₂ NP size distribution and laser wavelength were also shown to be related, with a smaller size distribution being associated with a lower wavelength. An X-ray diffraction examination revealed that the TiO₂ NP's structure is polycrystalline and has several peaks.

Keywords: Laser ablation, titanium dioxide, physical properties, XRD, TEM.

Introduction

The wide range of applications for nanocrystalline TiO₂NPs, including gas sensors, antibacterial coatings, photoelectric conversion in solar cells, and photocatalysis, is drawing a lot of interest in the material [1]. As a result, titanium dioxide is being researched extensively. TiO₂-photocatalysis is a great tool for environmental applications like the breakdown of organic pollutants [2]. In general, thin and powder films were the two main modes of TiO₂ application. Liquid and gas phase catalysis was the primary use of the older TiO₂form. Its phase composition and particle size were typically used to specify its photocatalytic activity [3]. Anatase, rutile, ilmenite, leucosene, perovskite, and sphene are among the approximately 45 distinct minerals that include titanium. Titanium dioxide (TiO₂) makes up about 90% of the minerals and is utilized as a white pigment in paints (69%), plastic (25%) and paper (5%). The remaining 1% is used in ceramics, coated and fabrics, roofing granules, printing ink, and floor coverings [4]. Titanium dioxide is composed of five polymorph phases: the stable phase, rutile



(tetragonal); TiO₂-II (orthorhombic) and TiO₂-III (hexagonal), two metastable high-pressure phases, and two metastable low-pressure phases, brookite (rhombohedral) and anatase (tetragonal), G. UH; which are particularly hard and can be artificially produced at very high pressure [5]. About 3.2 eV is the E_g of anatase, whereas 3.0 eV is the E_g of rutile. The rarest naturally occurring phase of titania is the third crystal phase, brookite, which is also the hardest to acquire in its purest form. As in previous stages, brookite is active via photocatalysis [6]. TiO₂ nanoparticles can be produced via a variety of techniques, such include milling, spray pyrolysis, sol-gel, chemical vapour deposition (CVD), and laser ablation. By rapidly reactively quenching ablated species at the plasma-liquid interface, laser ablation is a novel technology of fundamental relevance for fabricating TiO₂ nanoparticles suspended in liquid. It is a possible method for managing non-material production as well[7]. Pulsed laser deposition (PLD), a term used to describe the thin film preparation field, is one of the many uses for lasers nowadays [8]. (PLA) in liquid is one potential process for producing titanium dioxide in a very irregular and highly scattered form [9]. PLA has the following benefits: it is easy to use, can produce NPs in pure solvents without the requirement for precursors, and can be used to change the composition of the particles by altering the medium's composition, targets, and laser radiation parameters [10]. Nd:YAG laser ablation of metal plate TiO₂ at a wavelength of (1064,532) nm, a repetition rate of 9 Hz, and a pulse width of 15 ns was used to create synthetic TiO₂ NPs. We created colloidal TiO₂ NPs in a manner similar to [11] .we synthesized colloidal TiO₂ NPs by ablating a titanium target immersed in distilled water[11]. This work created TiO₂ nanoparticles with good dispersibility and homogeneous size.

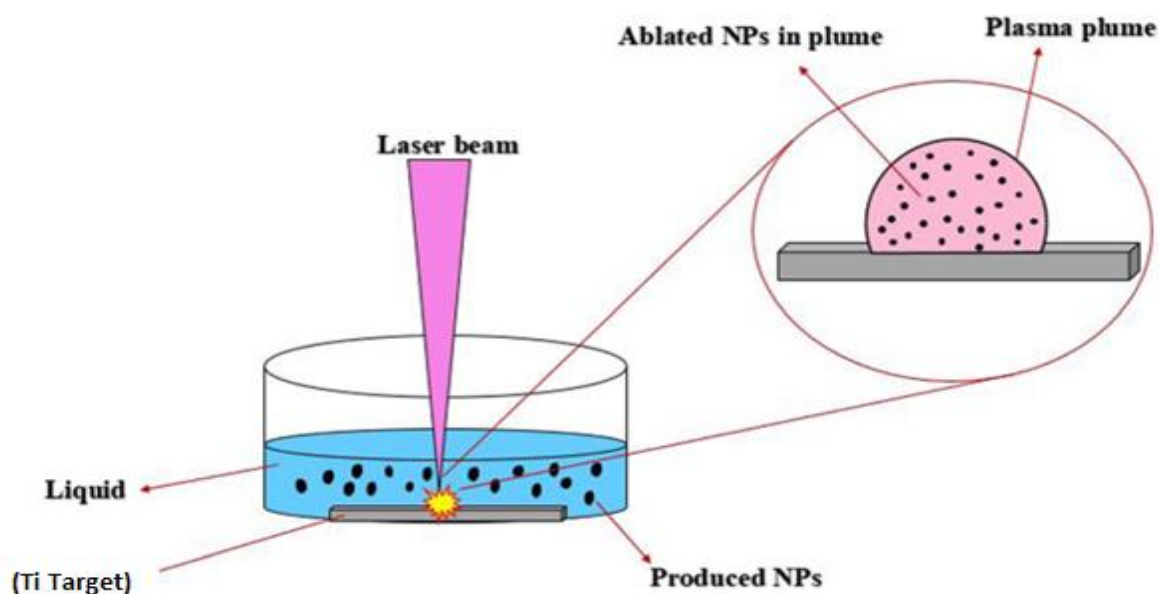
2. Preparation of TiO₂ NPs

Using a nanosecond pulsed laser, TiO₂NPs were synthesized in deionized water from an objective of 99.99% pure titanium (Ti). A titanium plate was positioned at the base of a glass vessel (refer to Figure 1), with the target being covered by around 10 milliliters of pure water. Table 1 shows the characteristics of a pulsed Q-switched Nd:YAG laser. For five minutes, the deionized water Ablation using laser procedure was conducted continuously. Once that was done, the PLA process began. The target was exposed to concentrated radiation using an LS2131M-20 Nd:YAG laser with a peak pulse energy of up to 300 mJ and a wavelength of (1064,532) nm. The repetition frequency and pulse duration were 9 Hz and 15 ns, respectively. Plasma plume is visible to the unaided eye when the Ti objective is exposed to laser light. This is because of the process of ablation.



Table-1. Laser parameters used in production of TiO₂NPs

The laser beam	Parameters	Value
	Wavelength (λ)	(1064,532) nm
	Rate of repetition	9HZ
	pulse duration	15 ns
	Diameter of beam	2.4 mm
	Laser pulse energy	(250,300) mJ
	No. of pulses	500 pulse
	Ablation time	15 minutes
Materials	Target	Ti metal
	Liquid	De-ionized water

**Figure- 1. An example of how a Ti target is laser-ablated in water[12].**

3. Results and discussion

3.1. UV-Visible Spectroscopy

In the wavelength scan area (200–1000 nm), the produced TiO₂ nanostructures' absorption spectra were recorded. The optical absorption spectra of TiO₂ nanostructures produced with a (1064,532)nm laser at different laser energies (250,300) mJ at 500 pulses during a 15-minute continuous ablation period are shown in Figure 2. With an increase in laser intensity, there was a noticeable rise in absorption in the 200–350 nm range, and the absorption edge migrated toward shorter wavelengths. Additionally, when laser energy increases, the intensity of the absorption peaks increases due to the high nanoparticle deposition.

The absorption behavior of TiO₂ NPs was also influenced by a wide range of factors, including size distribution, morphologies, and stoichiometry[13]. The explanation for this is that by applying more energy to the target, a stronger plume of plasma forms., and more material is ablated, resulting in a denser nanostructure.

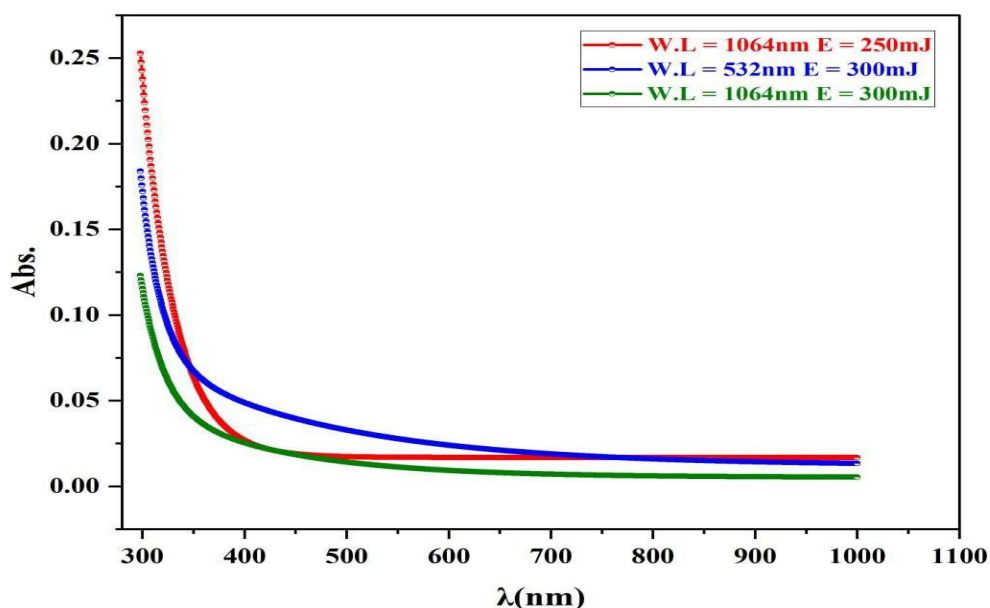


Figure -2. TiO₂ nanostructures generated at varying laser fluencies: UV-Vis absorbance spectra.

To determine the optical band gap of the generated NPs, Tauc's relation was applied according to [14].

$$(\alpha h\nu)^n = K(h\nu - E_g) \dots \dots \dots (1)$$

Where K is the effective mass constant. that connects to the bands of conduction and valence, $h\nu$ is photon energy, E_g is the optical band gap of NPs, and α is the absorption coefficient. Indicating the kind of electronic transition leading to absorption, the number n can have values of 2 or ½ based on whether the transition is direct or indirect. Once NPs' band gap in colloids is intersected along with the $h\nu$ -axis, it shows how the direct transition is made, a linear line representing $(\alpha h\nu)^2$ is drawn against $h\nu$. Because of the reduction in particle size brought about by quantum confinement and the increase in surface/volume ratio, TiO₂ NPs had band gap values of (3.26, 3.3, and 3.09) eV, which are greater than the bulk TiO₂ and correspond to TiO₂ NPs synthesized using (250, 300) mJ, respectively[15]. Figure 3 illustrates how the optical band gap narrows with increasing laser energy. The reduction in the value of the energy gap may be ascribed to forbidden contaminants, leading to energy gaps in donors at different levels in the vicinity of the band of conduction approaching those at lower energies. After ablating a

small number of TiO₂ nanoparticles from the target, 3.26 eV, 3.3 eV, and 3.09 eV were observed for the measured band gap energies at 250 mJ, 300 mJ, and 1064 nm wavelengths, respectively.

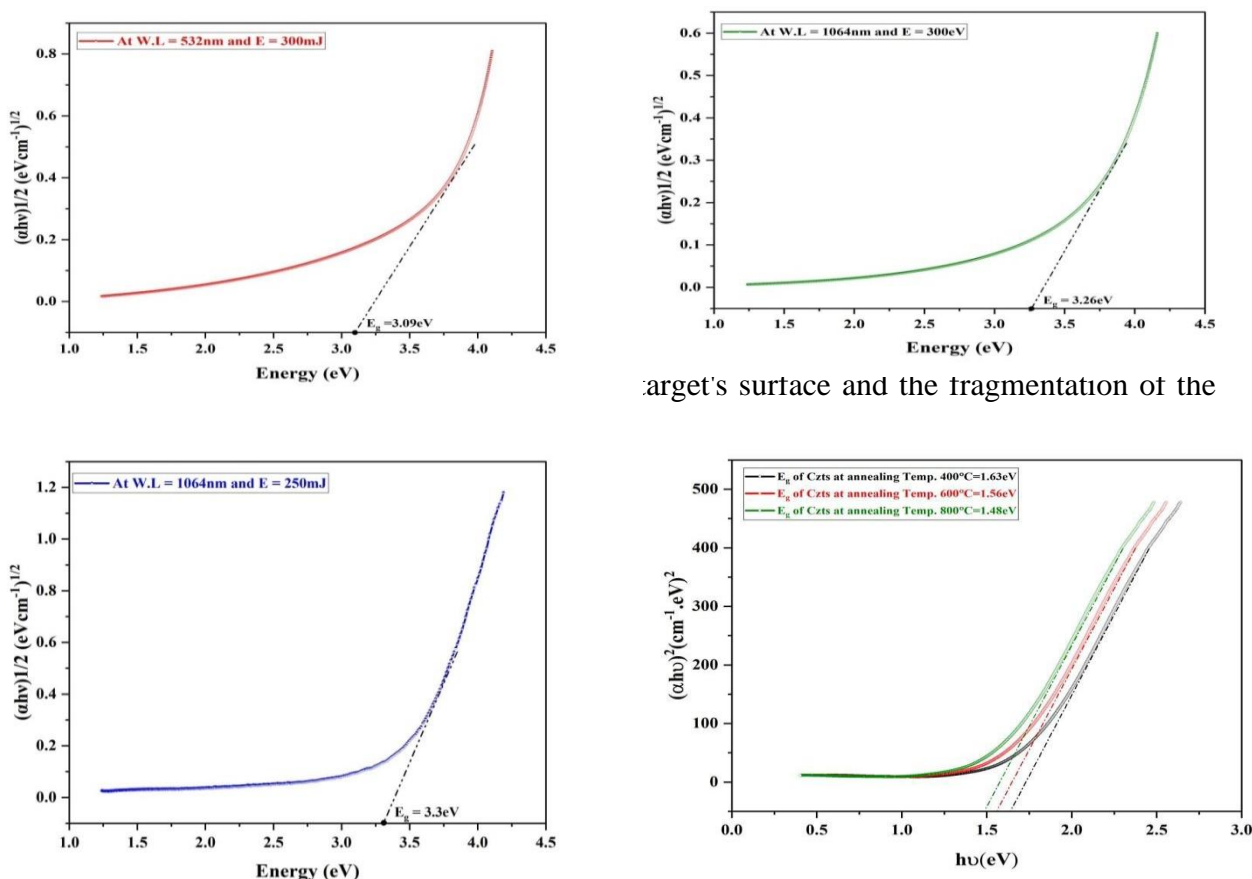


Figure- 3. The band gap in optical systems of titanium NPs at various laser energies and wavelengths prepared (250mJ, 300mJ)at wavelength 1064 and 300mJ at wavelength 532nm.

3.2 . X-ray Diffraction (XRD)

PLD is a highly significant method for creating nanostructured TiO₂ due to its contactless treatment. On treated surfaces, nanostructures in different patterns might be easily created without the need for additional masking. Figure 4 displays the prepared NPs' XRD patterns. Based on information released by the Joint Committee on Powder Diffraction Standards (JCPDS No21-1272), these planes corresponded with the crystal planes associated with the TiO₂ phase[17]. Ascribed to the (200) plane, the primary peak in the specimens' X-ray diffraction patterns is located at $2\theta=32^\circ$ and is the result of X-ray photons diffracting from the crystal lattice for the TiO₂ Brookite phase[18]. Due to the produced nanoparticles' low concentration and possible deposition on an amorphous glass substrate, the remaining peaks are absent when compared to the standard XRD diffraction pattern. Furthermore, the XRD pattern's widening confirmed the produced TiO₂ nanostructures' shrinkage in size.

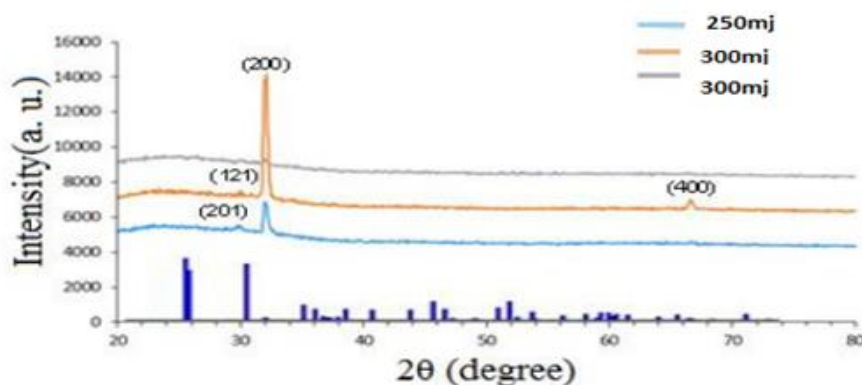


FIGURE -4. (XRD) OF TiO₂ NPs CREATED BY LASER-INDUCED PLASMA AT VARIOUS LASER WAVELENGTHS AND ENERGIES

3.3. Transmission Electron Microscope (TEM) imaging

The method most often used to examine the shape and form of the produced NPs is TEM. As seen in Figure 5, the synthesized NPs' shape was depicted by TEM and is consistent, nearly spherical. The particles' size and shape are controlled by the laser parameters as well as the surrounding liquid. A very thin metal coating is heated over the point of melting by the laser beam's interaction with the solvent-submerged Ti target. Because of the metal to liquid heat transition, the solvent layer next to it reaches a temperature that is almost identical and significantly higher than the liquid's boiling point at standard pressure. This is what led to the bubbles forming. Titanium oxide is produced as a byproduct of the reaction between the molten metal and oxygen from the evaporated solvent, which forms nanoparticles. A clear sign of the particles' quick cooling, which may have caused twinning, dislocations, and lattice imperfections, is that the two wavelengths showed that the titanium dioxide particles that were generated had different crystalline morphologies; some were obviously polycrystalline, while others were almost single-crystal with imperfections.

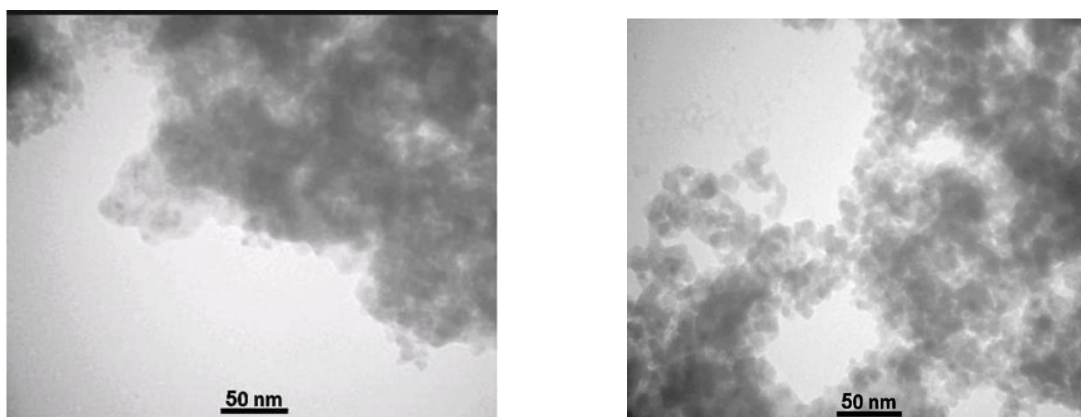


Figure -5. Transmission Electron Microscope images of the TiO₂ NPs created by ablating titanium submerged in 1064 nm and 532nm wavelength.

3.4 . Conclusion

In summary, by ablating the metal Ti target submerged in deionized water (PLAL) with a pulsed laser, we were able to successfully prepare TiO₂ nanoparticles with distinctive crystal synthesis. This technique is straightforward, adaptable, controllable, and less costly as a result of technology. Because of their optical properties, pure TiO₂ nanoparticles absorb light in a region of the UV spectrum that matches the UV light spectrum. When laser energy increased from 250–300 mJ, the energy band gap for titanium NPs fell from the 3.3 eV to 3.26 eV, respectively, at wavelength 1064 nm. And the energy band gap decreasing to 3.09 eV with the decreased of wavelength to 532 nm. Additionally, the as-prepared samples' crystal structure was discovered to be in a brookite phase by X-ray Diffraction analysis. There was some minor aggregation observed, and the particles have a spherical form.

References:

- [1] Boutinguiza, M., del Val, J., Riveiro, A., Lusquiños, et al., "Synthesis of titanium oxide nanoparticles by ytterbium fiber laser ablation," *Physics Procedia*, vol. 41, p. 787-793, 2013.
- [2] Ghaleb, A. M., Benkrima, Y., Munef, R. A., Shihatha, A. T., Megdoud, Y., & Ghaleb, Z. T. (2024). A FIRST-PRINCIPLES STUDY EFFECT PRESSURE OF ELECTRONIC AND OPTICAL PROPERTIES OF R-TiO₂. *Journal of Chemistry and Technologies*, 32(1), 9-16.
- [3] Ding, Z., Lu, G.Q. and Greenfield, P.F. 2000. "Role of the Crystallite Phase of TiO₂ in Heterogeneous Photocatalysis for Phenol Oxidation in Water", *Journal of Physical Chemistry B*, 104(2000): 4815-4820.
- [4] H. Park, Y. Park, W. Kim, W. Choi, Surface modification of TiO₂ photocatalyst for environmental applications, *J Photochem Photobiol C: Photochem Rev* 15 (2013) 1–20.
- [5] J.L. Murray, The O-Ti (Oxygen-Titanium) System, *Bulletin of Alloy Phase Diagrams* Vol. 8 No. 2 1987.
- [6] Zhu, T. and Gao, S.P., "The stability, electronic structure, and optical property of TiO₂ polymorphs," *The Journal of Physical Chemistry C*, vol. 118(21), p.11385-11396, 2014.
- [7] Zuñiga-Ibarra, V. A., Shaji, S., Krishnan, B., Johny, J., Kanakillam, S. S., Avellaneda, D. A., ... & Ramos-Delgado, N. A. (2019). Synthesis and characterization of black TiO₂ nanoparticles by pulsed laser irradiation in liquid. *Applied Surface Science*, 483, 156-164.
- [8] Falah A-H. Mutlak, 2014. "Photovoltaic enhancement of Si micro-and nanostructure solar cells via ultrafast laser texturing", *Turkish J. of physics*, 38(1): 2014.
- [9] E. D. Fakhrutdinova, A. V. Shabalina, M. A. Gerasimova, et al., *Materials*, 13, No. 9, Art. No. 2054 (2020).
- [10] N. Ali, Sh. Bashir, U. N. Begum, et al., *Appl. Surf. Sci.*, 405, 298 (2017).
- [11] Ibrahim, K. H., Salman, J. A., & Ali, F. A. (2009). Extracellular Biosynthesis of TiO₂ Nanoparticles Using Supernatant Culture of *Lactobacillus crispatus*. *Journal of Global Pharma Technology*, 11(07).
- [12] Abdollahi, M., Jaleh, B., Rashidian Vaziri, M. R., Arnaouty, W., & Varma, R. S. (2022). Good optical limiting performance of platinum nanoparticles prepared by laser ablation in a water environment. *Pramana*, 96(4), 166.



-
- [13] Ola, O., & Maroto-Valer, M. M. (2015). Review of material design and reactor engineering on TiO₂ photocatalysis for CO₂ reduction. *Journal of Photochemistry and Photobiology C: Photochemistry Reviews*, 24, 16-42.
- [14] Buraq, T. A. M. (2020). The use of laser ablation technique for the synthesis of titanium dioxide nanoparticles synergistic with sulfamethoxazole to prepare an anti-corrosion surface coating for mild steel and study of refraction and absorption. *International Journal of Corrosion and Scale Inhibition*, 9(3), 1025-1036.
- [15] Thamir, A. D., Haider, A. J., & Ali, G. A., "Preparation of Nanostructure TiO₂ at Different Temperatures by Pulsed Laser Deposition as Solar Cell," *Journal of Engineering Technology*, vol.34, p.193-204. 2016.
- [16] Aziz, W. J., Ali, S. Q., & Jassim, N. Z., "Production TiO₂ Nanoparticles Using Laser Ablation in Ethanol," *Silicon*, vol.10(5), p.2101-2107, 2018.
- [17] Acacia, N., Barreca, F., Barletta, E., Spadaro, D., Currò, G., & Neri, F. (2010). Laser ablation synthesis of indium oxide nanoparticles in water. *Applied Surface Science*, 256(22), 6918-6922.
- [18] Andrade-Guel, M., Díaz-Jiménez, L., Cortés-Hernández, D., Cabello-Alvarado, C., Ávila-Orta, C., Bartolo-Pérez, P., & Gamero-Melo, P. (2019). Microwave assisted sol-gel synthesis of titanium dioxide using hydrochloric and acetic acid as catalysts. *boletín de la sociedad española de cerámica y vidrio*, 58(4), 171-177.

